THE JOURNAL OF PHYSICAL CHEMISTRY C
A JOURNAL OF THE AMERICAN CHEMICAL SOCIETY

pubs.acs.org/JPCC

Article

Locating the Frequency of Turnover in Thin-Film Diffusion Impedance

Mathijs Janssen* and Juan Bisquert*

Cite This: J. Phys. Chem. C 2021, 125, 15737−15741

Read Online

ACCESS | Metrics & More | Article Recommendations

ABSTRACT: The impedance of diffusion is an important tool to investigate a wide variety of systems, including electrochemical devices such as Li-ion batteries, porous electrodes, and solar cells. The classical impedance model for diffusion in a thin layer with a blocking boundary contains two separate regimes: Warburg diffusion at high frequency and capacitive charging at low frequency. Here, we provide a physical criterion for the transition between these two regimes, as the point of closest approach between early- and late-time approximations of the exact diffusion current. The resulting frequency is $(\pi^2/2)\omega_d$ with respect to the natural frequency $\omega_d = D_n/L^2$, with D_n being the diffusion constant and L being the thickness of the layer.

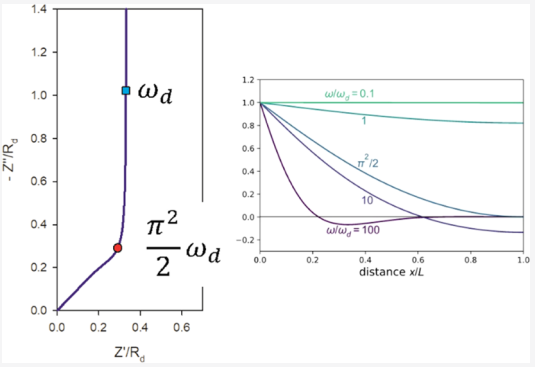

1. INTRODUCTION

Models for the impedance of spatially restricted diffusion are used to understand a large variety of technologies. Estimating the diffusion resistance and coefficient plays a vital role in the understanding and diagnostics of porous electrodes.[1−4] Earlier studies have used transmission line modeling based on impedance analysis for understanding electrode reaction kinetics and diffusion with temperature.[5−11] Another method is based on galvanostatic intermittent titration technique (GITT) experimental analysis.[12] Likewise, the impedance of diffusion-recombination, often determined by transmission line models, is widely used to understand the charging in semiconductor devices, solar cells,[13−15] and porous electrodes. The identification of characteristic frequencies of the impedance of electrochemical systems using both responses in the frequency and time domains has been treated extensively.[16,17] In particular, the identification of the frequency that marks the transition between diffusion in infinite space and capacitive charging of a film is an important problem that has been treated for decades.[6,13,15,18,19] Here, we provide a physical criterion to establish the frequency of transition in relation to the thin-film parameters.

2. RESTRICTED DIFFUSION IMPEDANCE

In diffusion in a thin layer in one dimension, charge carriers with concentration $n(x, t)$ are injected at $x = 0$ by an applied voltage $V(t)$ and travel by diffusion up to a boundary at $x = L$. The carrier flux $J_n(x, t)$ is defined by the concentration and average velocity v_n of the particles as

$$J_n = nv_n \tag{1}$$

The flux is related to the gradient of the concentration by

$$J_n = -D_n\frac{\partial n}{\partial x} \tag{2}$$

where D_n is the diffusion constant of the charge carriers. The conservation equation is

$$\frac{\partial n}{\partial t} = -\frac{\partial J_n}{\partial x} \tag{3}$$

Combining the last two equations, we obtain

$$\frac{\partial n}{\partial t} = D_n\frac{\partial^2 n}{\partial x^2} \tag{4}$$

We consider a blocking boundary condition $J_n(L, t) = 0$, so that diffusing particles are reflected at $x = L$. This choice yields a Neumann boundary condition on the carrier density $n(x, t)$

$$\frac{\partial n}{\partial x}(L, t) = 0 \tag{5}$$

The impedance as a function of the angular frequency ω is obtained by assuming $n(x, t)$ to be of the form $n(x, t) = n_0 + \tilde{n}(x,$

Received: May 25, 2021
Revised: June 25, 2021
Published: July 12, 2021

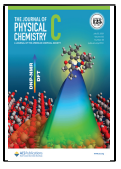

https://doi.org/10.1021/acs.jpcc.1c04572
J. Phys. Chem. C 2021, 125, 15737−15741

$\omega)e^{i\omega t}$, with $\tilde{n}(x, \omega)$ being a small perturbation around the background density n_0. In this case, eq 4 reduces to[13,15]

$$i\omega\tilde{n} = D_n\frac{\partial^2\tilde{n}}{\partial x^2} \tag{6}$$

The solution to eq 6 subject to eq 5 can be expressed as

$$\tilde{n}(x, \omega) = \tilde{n}(0, \omega)\frac{\mathrm{Cosh}\left(\frac{x-L}{\lambda(\omega)}\right)}{\mathrm{Cosh}\left(\frac{L}{\lambda(\omega)}\right)} \tag{7}$$

where $\tilde{n}(0, \omega)$ represents the carrier density at the contact at $x = 0$, and where λ is the penetration length defined as

$$\lambda(\omega) = \left(\frac{D_n}{i\omega}\right)^{1/2} \tag{8}$$

Importantly, the penetration length reaches the system size

$$|\lambda(\omega_d)| = L \tag{9}$$

when the driving frequency equals the characteristic frequency ω_d for diffusion across the layer

$$\omega_d = \frac{D_n}{L^2} \tag{10}$$

We rewrite the penetration length in terms of ω_d as

$$\lambda(\omega) = \frac{L}{z(\omega)} \tag{11}$$

where

$$z(\omega) = \left(\frac{i\omega}{\omega_d}\right)^{1/2} \tag{12}$$

In Figure 1, we plot the distribution of carriers in the ac perturbation at different angular frequencies. For $\omega/\omega_d = 100$,

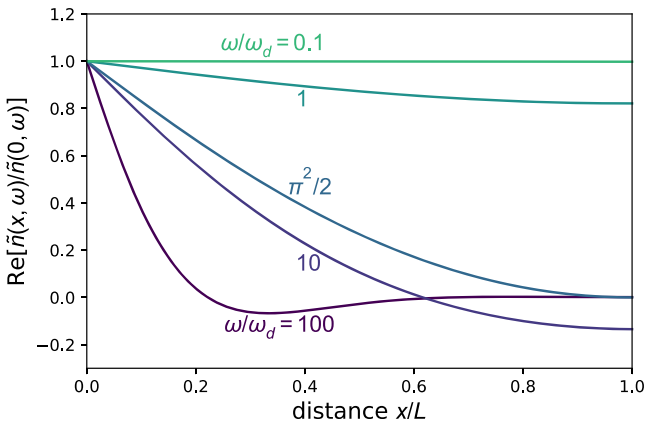

Figure 1. Plot of the real part of the carrier density $\hat{n}(x, \omega)$ [eq 7] at different values of ω/ω_d as indicated.

we observe that perturbations in $\tilde{n}(x, \omega)$ do not reach the boundary at $x = L$. Conversely, at $\omega/\omega_d = 0.1$, the film is filled homogeneously with carriers. Note that the shown concentration will be oscillating with time as $e^{i\omega t}$.

The carrier density $\tilde{n}(0, \omega)$ at the contact at $x = 0$ is a function of the applied voltage by some function $n(V)$ that depends on the film material properties. For the small perturbation applied voltage, we obtain the relationship

$$\tilde{V}(\omega) = \left(\frac{dn}{dV}\right)^{-1}\tilde{n}(0, \omega) \tag{13}$$

For a more compact expression, we relate the derivative in eq 13 to the chemical capacitance[20] (or intercalation capacitance,[8] in the case of Li-ion batteries) of the film C_μ, defined as

$$C_\mu = qL\frac{dn}{dV} \tag{14}$$

where q is the elementary charge. Then, we have the relation between ac applied potential and ac concentration at the injection boundary in the following form

$$\tilde{V}(\omega) = \frac{qL}{C_\mu}\tilde{n}(0, \omega) \tag{15}$$

We can now determine the impedance

$$Z = \frac{\tilde{V}}{\tilde{j}_e} \tag{16}$$

where $\tilde{j}_e(\omega) = q\tilde{J}_n(0, \omega)$ is the electrical current. With the carrier density $\tilde{n}(x, \omega)$ from eq 7 and the flux from eq 2, we find

$$Z(\omega) = \frac{R_d}{z(\omega)}\mathrm{Cotanh}[z(\omega)] \tag{17}$$

where the diffusion resistance R_d is given by

$$R_d = \frac{1}{\omega_d C_\mu} \tag{18}$$

The impedance in eq 17 is shown in Figure 2 in the complex plane plot. Equation 17 can also be derived from a transmission

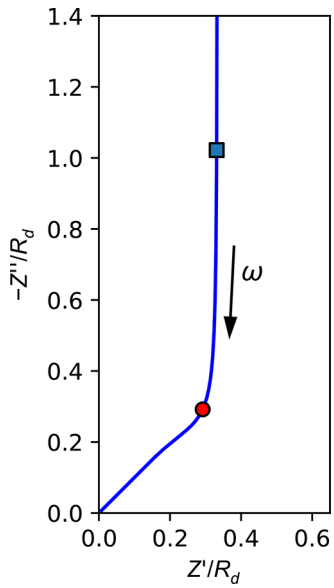

Figure 2. Spatially restricted diffusion impedance with blocking boundary [eq 17]. The square point indicates the angular frequency $\omega_g = \omega_d$ and the circle point is for $\omega_g = (\pi^2/2)\omega_d$.

line model, as shown in Figure 3.[13] The graph in Figure 2 shows two distinct domains of behavior. At high frequency, $\omega \gg \omega_d$, we have the Warburg impedance

https://doi.org/10.1021/acs.jpcc.1c04572
J. Phys. Chem. C 2021, 125, 15737−15741

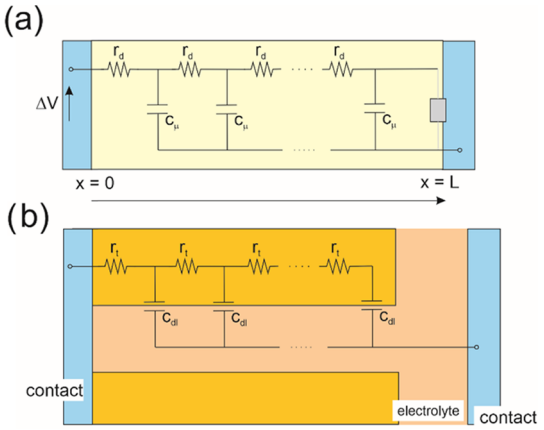

Figure 3. (a) Transmission line for diffusion in a thin layer with a distributed chemical capacitance c_μ and diffusion resistance r_d. The suggested element at $x = L$ is the specific impedance of the final boundary. For blocked diffusion, it is an open circuit; for an absorbing boundary, it is a short-circuit. The perturbation of voltage is imposed at the left electrode. (b) Transmission line model for a porous electrode filled with electrolyte with a distributed double-layer capacitance c_{dl} and transport resistance r_t.

$$Z(\omega) = R_d \frac{\lambda(\omega)}{L} = R_d \left(\frac{i\omega}{\omega_d}\right)^{-1/2} \tag{19}$$

It has an inclination of 45° in the complex plot. In this domain, the injected charge only penetrates the film to a limited extent, $|\lambda(\omega)| < L$, as shown in Figure 1.

At low frequency, $\omega \ll \omega_d$, eq 17 traces a vertical line that is approximated by the expression

$$Z(\omega) = \frac{1}{3}R_d + \frac{1}{i\omega C_\mu} \tag{20}$$

The total resistance of the transmission line is reduced by a factor of 1/3. Here, $|\lambda(\omega)| > L$, the concentration is homogeneous, and the oscillations of injected charge simply charge and discharge the chemical capacitor. It is important to remark that the chemical capacitance is distributed over the whole length, as shown in the transmission line model. The vertical line in Figure 2 does not correspond to the final boundary. If a surface capacitance at the final boundary exists, it needs to be added as another element, as indicated in Figure 3a by a gray element and described in the literature.[2,21]

3. FREQUENCY OF TURNOVER

In between the impedance lines at 45° and 90°, there is a turnover region or "ankle" that corresponds to the arrival of the ac signal to the boundary of the space, as $|\lambda(\omega)|$ grows as the frequency decreases. In impedance spectroscopy studies, the frequency ω_g (g stands for graphical) at which this turnover takes place is normally identified with ω_d [eq 10], the frequency of diffusion across the layer. This frequency is then used to experimentally determine the diffusion coefficient, by fitting the measured turnover frequencies with respect to $1/L^2$ in a series of samples of different thicknesses.[22] Yet, if we plot the naturally defined value ω_d in Figure 2 (square point), we obtain that it lies very far away from the ankle. Hence, experimental determination of D_n based on identifying ω_d as the frequency of the ankle will seriously underestimate the value of D_n.

Over the years, different criteria for the frequency of turnover have been suggested.[6,13,15,18,19] Armstrong[18] proposed $\omega_g = 5.12\ \omega_d$ and Cabanel et al.[6] used $\omega_g = 3.88\ \omega_d$. These criteria were developed from the geometrical properties of the impedance $Z(\omega)$, e.g., by taking a specific value of the derivative of the Z-line in the complex plane. In the description of the diffusion-recombination impedances calculated by Bisquert, $\omega_g = 2\pi\omega_d = 6.28\ \omega_d$ was taken,[13,15] which was also an arbitrary value. Notably, all of the suggested points locate the transition at a frequency that is above ω_d by a factor of about 5, but none of them has been adopted generally since they lack a physical interpretation.

Here, we aim to establish a physical criterion for the location of ω_g that we can take as a suitable boundary between the two limiting ω/ω_d behaviors. We note from the outset that the definition is arbitrary to some extent. The transition region is a curved graph, and there is no single instant that we can point out as the boundary. Yet, there must be some physical reason for the ankle being located around the frequency at which it appears.

Given the definition $Z(\omega) = \tilde{V}/\tilde{j}_e$, a transition of $Z(\omega)$ in the frequency domain can be expected to be related to a transition of $j_e(t)$ in the time domain. Accordingly, to study $J_n(x, t)$ in the time domain, we consider the same diffusion eq 4 with the blocking boundary condition eq 5, but now subject to a step $n(0, t) = n_0$ and for the initial condition $n(x, 0) = 0$. This set of equations is equivalent to a heat diffusion problem discussed by Carslaw and Jaeger,[23] eq 6 on p. 313 (albeit for flipped boundary conditions). Replacing $x \to L - x$ in their solution, we readily find

$$\frac{n(x, t)}{n_0} = 1 - 2\sum_{m=1}^{\infty} \beta_m^{-1} \sin\left(\beta_m \frac{x}{L}\right) \exp\left(-\beta_m^2 \frac{D_n t}{L^2}\right) \tag{21}$$

where $\beta_m = \pi(m - 1/2)$ with $m = 1, 2, \ldots$ Hence, the carrier flux measured at the injection point follows with eq 2 as

$$J_n(0, t) = \frac{2n_0 D_n}{L} \sum_{m=1}^{\infty} \exp\left(-\beta_m^2 \frac{D_n t}{L^2}\right) \tag{22}$$

At late times $t > L^2/D_n$, only the $m = 1$ term in the above sum contributes substantially, and $J_n(0, t)$ is decently approximated by

$$J_n(0, t) = \frac{2n_0 D_n}{L} \exp\left(-\frac{\pi^2}{4}\omega_d t\right) \tag{23}$$

Conversely, at early times, diffusion is hardly affected by the blocking boundary at $x = L$, and we may solve eq 4 in a semi-infinite geometry $x \in [0, \infty)$ instead, yielding (ref 24, eq 3.14 on p. 167)

$$n(x, t) = n_0 \operatorname{Erfc}\left(\frac{x}{\sqrt{4D_n t}}\right) \tag{24}$$

For this early-time response, corresponding to spatially unrestricted diffusion, the flux at the injection point reads

$$J_n(0, t) = \frac{n_0 D_n}{L} \frac{1}{\sqrt{\pi\omega_d t}} \tag{25}$$

In Figure 4a, we plot the full solution of the carrier flux in eq 22 as well as the short- and long-time approximations. We see that for long times the full solution is decently approximated by eq 23, while for early times eq 22 is well approximated by eq 25. We can determine the time t_g for which eqs 23 and 25 approach

https://doi.org/10.1021/acs.jpcc.1c04572
J. Phys. Chem. C 2021, 125, 15737−15741

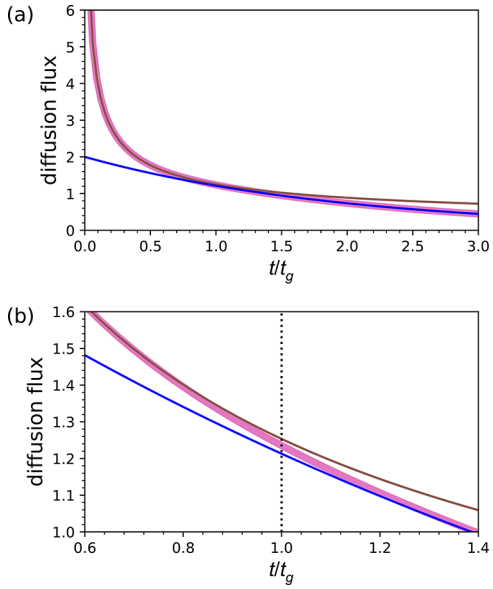

Figure 4. Diffusion flux $J_n(0, t)$ for injected charge at $x = 0$, as a function of time. We show the full solution, eq 22, with a thick pink line; approximations for late and early times, eqs 23 and 25, are shown with thin blue and brown lines, respectively. Panel (b) is a zoom-in of panel (a), showing more clearly the point of closest approach between the two approximations, with which we defined the time constant $t_g = (\pi^2\omega_d/2)^{-1}$.

each other the closest, by setting the time derivative of the difference between those equations to zero

$$\frac{d}{dt}\left[2\exp\left(-\frac{\pi^2}{4}\omega_d t\right) - \left(\frac{1}{\pi\omega_d t}\right)^{1/2}\right] = 0 \tag{26}$$

which yields the transcendental equation

$$\pi^{5/2}\exp\left(-\frac{\pi^2}{4}\omega_d t_g\right) = \left(\frac{1}{\pi\omega_d t_g}\right)^{1/2} \tag{27}$$

Equation 27 is solved by $t_g = 0.209424\ \omega_d^{-1}$, which is very close to (but not exactly) $2/\pi^2 = 0.20264$. The closest approach at this point is illustrated in Figure 4b by a dashed vertical line. We interpret this time scale t_g to be the time that marks the transition between the two separate behaviors, semi-infinite diffusion and charge accumulation, in the impedance spectra. Therefore, we suggest defining the turnover frequency by

$$\omega_g = \frac{\pi^2}{2}\omega_d = 4.935\omega_d \tag{28}$$

This ω_g is plotted with a red circle in Figure 2. This circle marks the turnover very well, as expected, and contains a clear physical criterion for the representation of diffusion impedances. Furthermore, applying the factor in eq 28 allows for the direct identification of the diffusion coefficient from the frequency of the ankle from impedance spectroscopy measurements.

4. CONCLUSIONS

In summary, the frequency of turnover in the restricted diffusion impedance contains important information. It relates to the diffusion coefficient and film thickness. One way to obtain these parameters is by a least-square fit of the full analytical impedance function to experimental data over a large frequency range. However, it is also useful to have a clear idea of the relation of the turnover to the characteristic frequency of diffusion, which enables one to obtain the same parameters by direct inspection. Another reason for clarifying the interpretation of the turnover is to compare diffusional systems that have different characteristic frequencies. We established a clear criterion for the interpretation of the ankle. Our method required analyzing the transient diffusion flux at short and long times separately and determining the time at which they approached each other the closest. For the frequency of turnover, we proposed the corresponding frequency $(\pi^2/2)\omega_d$, which serves as a robust criterion for the interpretation of the different parts of the diffusion impedance.

AUTHOR INFORMATION

Corresponding Authors

Mathijs Janssen − *Department of Mathematics, Mechanics Division, University of Oslo, N-0851 Oslo, Norway*; Email: mathijsj@math.uio.no

Juan Bisquert − *Institute of Advanced Materials (INAM), Universitat Jaume I, 12006 Castelló, Spain*; orcid.org/0000-0003-4987-4887; Email: bisquert@uji.es

Complete contact information is available at: https://pubs.acs.org/10.1021/acs.jpcc.1c04572

Notes

The authors declare no competing financial interest.

ACKNOWLEDGMENTS

We thank the financial support by Generalitat Valenciana under project PROMETEO/2020/028.

REFERENCES

(1) de Levie, R. On porous electrodes in electrolyte solutions. *Electrochim. Acta* **1963**, *8*, 751−780.

(2) Bisquert, J. Influence of the boundaries in the impedance of porous film electrodes. *Phys. Chem. Chem. Phys.* **2000**, *2*, 4185−4192.

(3) Paasch, G.; Micka, K.; Gersdorf, P. Theory of the electrochemical impedance of macrohomogeneous porous electrodes. *Electrochim. Acta* **1993**, *38*, 2653−2662.

(4) Janssen, M. Transmission line circuit and equation for an electrolyte-filled pore of finite length. *Phys. Rev. Lett.* **2021**, *126*, No. 136002.

(5) Ho, C.; Raistrick, I. D.; Huggins, R. A. Application of a-c techniques to the study of lithium diffusion in tungsten trioxide films. *J. Electrochem. Soc.* **1980**, *127*, 343−350.

(6) Cabanel, R.; Barral, G.; Diard, J.-P.; Le Gorrec, B.; Montella, C. Determination of the diffusion coefficient of an inserted species by impedance spectroscopy: application to the $H/H_x\ Nb_2O_5$ system. *J. Appl. Electrochem.* **1993**, *23*, 93−97.

(7) Montella, C. EIS study of hydrogen insertion under restricted diffusion condictions. I. Two-step insertion reaction. *J. Electroanal. Chem.* **2001**, *497*, 3−17.

(8) Levi, M. D.; Aurbach, D. Frumkin intercalation isotherm - a tool for the elucidation of Li ion solid state diffusion into host materials and charge transfer kinetics. A review. *Electrochim. Acta* **1999**, *45*, 167−185.

(9) Huang, J. Diffusion impedance of electroactive materials, electrolytic solutions and porous electrodes: Warburg impedance and beyond. *Electrochim. Acta* **2018**, *281*, 170−188.

(10) Primdahl, S.; Mogensen, M. Gas diffusion impedance in characterization of solid oxide fuel cell anodes. *J. Electrochem. Soc.* **1999**, *146*, 2827−2833.

(11) Rangarajan, S. P.; Barsukov, Y.; Mukherjee, P. P. In operando impedance based diagnostics of electrode kinetics in Li-ion pouch cells. *J. Electrochem. Soc.* **2019**, *166*, A2131−A2141.

(12) Verma, A.; Smith, K.; Santhanagopalan, S.; Abraham, D.; Yao, K. P.; Mukherjee, P. P. Galvanostatic intermittent titration and performance based analysis of $LiNi_{0.5}Co_{0.2}Mn_{0.3}O_2$ Cathode. *J. Electrochem. Soc.* **2017**, *164*, A3380−A3392.
(13) Bisquert, J. Theory of the impedance of electron diffusion and recombination in a thin layer. *J. Phys. Chem. B* **2002**, *106*, 325−333.
(14) Wang, Q.; Ito, S.; Grätzel, M.; Fabregat-Santiago, F.; Mora-Seró, I.; Bisquert, J.; Bessho, T.; Imai, H. Characteristics of high efficiency dye-sensitized solar cells. *J. Phys. Chem. B* **2006**, *110*, 25210−25221.
(15) Bisquert, J.; Mora-Sero, I.; Fabregat-Santiago, F. Diffusion-recombination impedance model for solar cells with disorder and nonlinear recombination. *ChemElectroChem* **2014**, *1*, 289−296.
(16) Hirschorn, B.; Orazem, M. E.; Tribollet, B.; Vivier, V.; Frateur, I.; Musiani, M. Determination of effective capacitance and film thickness from constant-phase-element parameters. *Electrochim. Acta* **2010**, *55*, 6218−6227.
(17) Moya, A. A. Identification of characteristic time constants in the initial dynamic response of electric double layer capacitors from high-frequency electrochemical impedance. *J. Power Sources* **2018**, *397*, 124−133.
(18) Armstrong, R. D. Impedance plane display for an electrode with diffusion restricted to a thin layer. *J. Electroanal. Chem. Interfacial Electrochem.* **1986**, *198*, 177−180.
(19) Cruz-Manzo, S.; Greenwood, P. Frequency transition from diffusion to capacitive response in the blocked-diffusion warburg impedance for EIS analysis in modern batteries. *J. Electrochem. Soc.* **2020**, *167*, No. 140507.
(20) Bisquert, J. Chemical capacitance of nanostructured semiconductors: its origin and significance for heterogeneous solar cells. *Phys. Chem. Chem. Phys.* **2003**, *5*, 5360−5364.
(21) Bisquert, J.; Garcia-Belmonte, G.; Bueno, P. R.; Longo, E.; Bulhões, L. O. S. Impedance of constant phase element (CPE) -blocked diffusion in film electrodes. *J. Electroanal. Chem.* **1998**, *452*, 229−234.
(22) Peng, W.; Aranda, C.; Bakr, O. M.; Garcia-Belmonte, G.; Bisquert, J.; Guerrero, A. Quantification of ionic diffusion in lead halide perovskite single crystals. *ACS Energy Lett.* **2018**, *3*, 1477−1481.
(23) Carlslaw, H. S.; Jaeger, J. C. *Conduction of Heat in Solids*, 2nd ed.; Oxford U. P.: Oxford, 1959.
(24) Cole, K. D.; Beck, J. V.; Haji-Sheikh, A.; Litkouhi, B. *Heat Conduction Using Green's Functions*, 2nd ed.; Taylor & Francis, 2010.

https://doi.org/10.1021/acs.jpcc.1c04572
J. Phys. Chem. C 2021, 125, 15737−15741